

Available online at www.sciencedirect.com

ScienceDirect

journal homepage: www.elsevier.com/locate/AJPS

Original Research Paper

Study of penetration mechanism of labrasol on rabbit cornea by Ussing chamber, RT-PCR assay, Western blot and immunohistochemistry



Pan Guo^{a,b,1}, Nan Li^{a,b,1}, Lili Fan^{a,b}, Jun Lu^c, Boying Liu^{a,b}, Bing Zhang^{a,b}, Yumei Wu^{a,b}, Zhidong Liu^{a,b,*}, Jiawei Li^{b,**}, Jiaxin Pi^{a,b}, Dongli Qi^{a,b}

^aTianjin State Key Laboratory of Modern Chinese Medicine, The Institute of Traditional Chinese Medicine, Tianjin University of Traditional Chinese Medicine, No. 88 Yuquan Road, Tianjin 300193, China

^bEngineering Research Center of Modern Chinese Medicine Discovery and Preparation, Tianjin University of Traditional Chinese Medicine, No. 88 Yuquan Road, Tianjin 300193, China

^cSchool of Pharmaceutical Science and Technology, Tianjin University, Tianjin 300193, China

ARTICLE INFO

Article history:

Received 10 November 2017
Revised 2 April 2018
Accepted 20 May 2018
Available online 15 June 2018

Keywords:

Enhanced corneal permeation
Tight junctions associated proteins
Labrasol
Ussing chamber
Western blot
Immunohistochemistry

ABSTRACT

Labrasol, as a non-ionic surfactant, can enhance the permeation and absorption of drugs, and is extensively used in topical, transdermal, and oral pharmaceutical preparations as an emulsifier and absorption enhancer. Recent studies in our laboratory have indicated that labrasol has a strong absorption enhancing effect on different types of drugs *in vitro* and *in vivo*. This study was performed to further elucidate the action mechanism of labrasol on the corneal penetration. In this research, the fluorescein sodium, a marker of passive paracellular transport of tight junction, was selected as the model drug to assess the effect of labrasol on *in vitro* corneal permeability. To investigate the continuous and real-time influence of labrasol on the membrane permeability and integrity, the Ussing chamber system was applied to monitor the electrophysiological parameters. And, furthermore, we elucidated the effect of labrasol on excised cornea at the molecular level by application of RT-PCR, Western blot, and immunohistochemical staining. The results indicated that labrasol obviously enhance the transcorneal permeability of fluorescein sodium, and the enhancement was realized by interacting with and down-regulating the associated proteins, such as F-actin, claudin-1 and β -catenin, which were contributed to cell-cell connections, respectively.

© 2018 Shenyang Pharmaceutical University. Published by Elsevier B.V.

This is an open access article under the CC BY-NC-ND license.

(<http://creativecommons.org/licenses/by-nc-nd/4.0/>)

* Corresponding author. Tianjin State Key Laboratory of Modern Chinese Medicine, The Institute of Traditional Chinese Medicine, Tianjin University of Traditional Chinese Medicine, No. 88 Yuquan Road, Tianjin 300193, China. Tel.: +86 22 59596170.

** Corresponding author. Engineering Research Center of Modern Chinese Medicine Discovery and Preparation, Tianjin University of Traditional Chinese Medicine, No. 88 Yuquan Road, Tianjin 300193, China. Tel.: +86 22 59596170.

E-mail addresses: lonerliuzd@163.com (Z.D. Liu), lijawei1981@163.com (J.W. Li).

¹ The two authors contributed equally to this work.

Peer review under responsibility of Shenyang Pharmaceutical University.

1. Introduction

It is widely known that cornea is the major site of drug absorption via intraocular drug delivery. Cornea has a multilayered structure, which can be mainly divided into epithelium, stroma and endothelium, and each layer offers a different polarity and a potential rate-limiting structure for drug permeation. Hence, the cornea is a relatively independent organ with a complete and complex barrier system for protecting the ocular structures from external substances. The corneal epithelium is natural lipoidal, containing 90% of the total cells in the cornea, and poses a significant resistance to the permeation of topically administered hydrophilic drugs [1]. The optimum candidates that could transport across the cornea readily are lipophilicity drugs, which are in the range of 10–100 when reflected by its n-octanol/buffer partition coefficient (PC) [2]. A lot of potentially therapeutic compounds, however, were limited to gain access to their sites of action due to the poor corneal permeability and failed to reach effective treatment because of the low bioavailability, which were the major challenges for treating ocular illnesses. To solve these problems, a lot of researches have been carried out to improve the corneal permeability of drugs. Generally, there are two approaches involved in improving the bioavailability of drugs and promoting cornea absorption. In the first way, drugs were modified as pro-drugs to alter their properties or processed into more advanced dosage forms by the application of modern pharmaceutical technology, such as liposome, nanoparticle, microemulsion, micelle and vesicle, etc. Penetration enhancers were required in the second method, such as nonionic surfactants Polyoxyethylene-9-lauryl ether [3], D-Alpha-tocopheryl poly (ethylene glycol) 1000 succinate (VE-TPGS) [4], solvents azone [5], ethyl alcohol, traditional Chinese medicines borneol [6], menthol [7], volatile oil and so on.

Labrasol, a nonionic surfactant containing saturated polyglycolysed C₈–C₁₀ glycerides with perfect solubilization effect, can promote the transdermal permeation and absorption of drugs with different polarity. It can also improve the dispersion stability of drugs and help self-emulsifying in water phase to form fine dispersed self-microemulsifying drug delivery systems [8]. Thus labrasol is widely applied as emulsifier and penetration promoter in all kinds of drug delivery systems. In addition, labrasol has an excellent biocompatibility and shows high tolerance and low toxicity in animals, of which LD₅₀ is 22 g/kg for rats by oral administration [9]. The toxicity and irritation of labrasol to eye tissues had been carried out in our previous studies, which indicated non-irritation and nontoxicity at the concentrations studied (0.5% - 8.0%, v/v). As a pharmaceutical excipient, labrasol has been recorded in European pharmacopoeia and American pharmacopoeia. Labrasol has been extensively studied to enhance transepithelial permeability for different substances. In the *in situ* absorption studies, Lin Y et al. found that labrasol (0.1%, v/v) could significantly enhance the intestinal absorption of rhodamine123 in rats, although the absorption enhancing effect of labrasol was much less than that of verapamil [10]. Our previous study also demonstrated that, with the concentration of labrasol increased from 1.5% to 3.0% (v/v), the permeability of baicalin through the excised rabbit cornea was

significantly enhanced [11]. Furthermore, Huang L et al. integrated borneol or menthol with labrasol and found that the penetrating effects were significantly increased by combining the application of labrasol with menthol or borneol. Among the various combined penetration enhancers, 0.1% borneol with 2% labrasol achieved the best apparent permeability, approximately 16.35 times that of the control [12].

The hydrophilic marker compound fluorescein sodium, which is transported passively through paracellular pathway, is commonly used as a fluorescent probe to observe the permeability of all sorts of physiologic barriers or the passive paracellular transport of tight junction [13,14]. The permeation amount of fluorescein sodium is determined by the corneal epithelium, which in return reflects the degree of integrity of epithelial tissues.

A great deal of studies demonstrated that the paracellular pathway permeability is limited primarily by the interactions of epithelial cells with each other and the extracellular matrix via the apical junctional complexes, which are composed of four kinds of connections: the tight junctions, adherens junctions, desmosomes and gap junctions [15]. The cytoskeleton, composed of the actin cytoskeleton, the microtubule network and the intermediate filaments, play a central role in maintenance of the morphological structure of epithelial cells. The actin cytoskeleton is a dynamic structure with continuous directional polymerization and disassembly, and the polymers are known as filamentous actin (F-actin) [16]. F-actin appears to be the major cytoskeletal components influencing tight junction permeability [17], which is closely connected with adherens junctions.

Tight junctions comprise of a series of different transmembrane proteins, such as occludins, claudins, junctional adhesion molecules (JAMs) and tricellulin, as well as increasing numbers of their scaffold proteins [18]. The classical functions of tight junctions are the regulation of paracellular permeability and the formation of an apical-basolateral intramembrane diffusion barrier that helps to maintain cell-surface polarity [19–21]. Moreover, paracellular permeability may differ greatly between diverse tissue barriers, depending on the composition of the expressed tight junction proteins and their expression level [22]. The claudins are transmembrane proteins with two extracellular loops and four transmembrane domains, which consist of at least 24 members ranging from 20 to 27 kDa. What is more, claudins directly regulate the gate function as paracellular tight junction channels (PTJC) by the sealing claudins. Claudin-1, in particular, contributes to paracellular sealing [23]. In addition to claudins, JAMs are a family of adhesion molecules also found in intercellular junctions, which are implicated in a variety of cellular process. For example, in studies by Liu Y et al., the antibodies to JAM-1 were found for the first time to express inhibition effect on the recovery of epithelial barrier function after transient calcium depletion, showing a direct evidence of JAM involvement in the regulation of barrier function of human epithelial monolayers [24].

The adherens junctions perform multiple functions including initiation and stabilization of cell-cell adhesion, regulation of the actin cytoskeleton, intracellular signaling and transcriptional regulation [25]. β -catenins are member of cytoplasmic proteins termed catenins that participate in the

formation, maintenance and function of adherens junctions [26]. Despite of the differences in proteins, structures and functions, adherens junctions and tight junctions regulate and interact with the actin cytoskeleton, respectively [27]. Co-ordinated interactions of all these constituents above-mentioned are pivotal for the regulation and maintenance of intercellular tight junctions. Therefore, the changes of these proteins expression indirectly reflect the integrity of tight junction.

Despite the large numbers of studies on enhancement of absorption and penetration through epithelial, its effect on rabbit corneal tight junctions was less characterized. For this reason, the present study was aimed to provide an insight into the potential mechanism of labrasol for the enhancement of *in vitro* rabbit corneal permeability. We evaluated the permeability of model drug fluorescein sodium by the utilization of Ussing chamber, in parallel with the measurement of transepithelial electrical resistance of rabbit cornea tissues. To further reveal the potential molecular mechanisms which were involved in the improvement of corneal permeability for model drug, the pre-treated tissue samples were then analyzed by RT-PCR and Western blot at molecular level. The changes in expressions of proteins which contribute to integrity of the epithelial tissue was confirmed and then further proved by immunohistochemical staining results eventually. Accordingly, it could be assumed that the enhancement of labrasol on the permeability of rabbit cornea *in vitro* for the selected substance was realized through the mechanism of tight junctions opening.

2. Materials and methods

2.1. Materials

Fluorescein sodium, oxidized glutathione and peroxidase-conjugated secondary antibodies were purchased from Sigma-Aldrich (Shanghai) Trading Co., Ltd. (Shanghai, China). Labrasol was purchased from Gattefosse (Shanghai) Trading Co., Ltd. (Shanghai, China). Agarose, UNI-Q-10 column total RNA extraction kit, total protein extraction kit, tris base, SDS, TEMED and 40% acrylamide solution were obtained from Sangon Biotech (Shanghai) Co., Ltd. (Shanghai, China). Transcriptor First Strand cDNA short Kit, FastStart Universal SYBR Green Master (ROX) and DAPI were purchased from Roche Diagnostics (Shanghai) Co. Ltd. (Shanghai, China). BCA protein quantitative analysis kit, PageRuler Unstained Protein Ladder and ECL Western Blotting Substrate were purchased from Thermo Fisher Scientific (China) Co., Ltd. (Shanghai, China). Rabbit claudin-1 antibodies, rabbit JAM-A antibodies were purchased from Aviva Systems Biology, Corp. (San Diego, CA, USA). Rabbit F-actin antibodies, rabbit β -catenin antibodies, rabbit GAPDH antibodies were purchased from Abcam PLC (Cambridge, UK). PVDF ProBlot membrane was purchased from Merck Millipore Corporation (Darmstadt, Germany). CY3-conjugated goat anti-rabbit (β -catenin) and CY3-conjugated goat anti-mouse (F-actin) were obtained from Jackson ImmunoResearch Laboratories, Inc. (West Grove, PA, USA). All other reagents were of analytical grade and were offered by our laboratory.

2.2. Animals

New Zealand albino rabbits weighting 2.0–2.5 kg, male and female unlimited, were used for the determination of *in vitro* corneal permeability, and were provided by Tianjin university of Traditional Chinese Medicine (TUTCM) animal experiment center. The animals were supplied with plenty of food and water and housed in standard cages in a light-controlled room at 25 ± 1 °C. All procedures involving the animals used in the present study were approved by TUTCM's Institutional Animal Care and Use Committee (IACUC) (January 9, 2013 (document number TCM-LAEC2013009)) and were consistent with the guidelines set by the National Institutes of Health (NIH publication no. 85–23, revised 1985).

2.3. Methods

2.3.1. Ussing chamber experiments

All animals were divided into five groups: the blank group (GBR solution), the control group (fluorescein sodium), 0.5% labrasol group (fluorescein sodium with 0.5% labrasol), 2.0% labrasol group (fluorescein sodium with 2.0% labrasol) and 8.0% labrasol group (fluorescein sodium with 8.0% labrasol).

After sacrificing, the freshly excised rabbit corneas with 2 mm sclera ring were gently mounted in the sample clip, and then were inserted vertically between the two halves of Ussing chambers (EM-CSYS-8, Physiologic Instruments, USA). The donor compartment (epithelium side) and the receiver compartment (endothelium side) were each filled with 5 ml GBR solution, and were continuously aerated with gas mixture (95% O₂ and 5% CO₂) to maintain the activity of cornea and balance the liquid. The corneas were stimulated by a continuous electric current pulse of 10 mV for 0.2 s every 1 min, and real-time monitoring for the electrical parameters of cornea was controlled by LabChart7 software. When the electric parameters were basically stable, the total liquid in both sides were withdrawn. Immediately, 5 ml of the GBR solution, fluorescein sodium solution and fluorescein sodium containing different concentrations of labrasol were added to the donor compartment, respectively and simultaneously, while the sample volume in the receiver compartment was replaced with fresh preheated GBR. At fixed intervals of 10 min, 300 μ l samples were taken from the receiver chamber and equal volume of GBR solution were supplemented, and samples collection continued to 240 min. During the penetration experiment, viability of tissue was routinely checked by measuring the electrical resistance every 1 min, as the main parameter for assessing monolayer integrity. Samples were analyzed by microplate reader to detect the fluorescence intensity.

The apparent permeability coefficient (Papp, cm/s) was calculated as follows:

$$P_{app} = \Delta Q / (\Delta t \cdot C_0 \cdot A \cdot 3600)$$

C₀ means the initial concentration of drugs in the donor compartment; A means the available area of 0.50 cm²; $\Delta Q/\Delta t$ could be obtained by calculating the slope of the steady-state part of accumulative penetration amount-time curve.

Transepithelial electrical resistance (TEER) is the important parameter that reflects the permeability and the activity of

Table 1 – The Real-time PCR oligonucleotide primers.

Primer name	Accession number	Primer	Sequence (5'–3')	PCR product (bp)
Rabbit GAPDH	NM_001082253.1	Forward	ATCACTGCCACCCAGAAGAC	146
		Reverse	GTGAGTTTCCCGTTCAGCTC	
Rabbit Claudin-1	NM_001089316.1	Forward	TGCATGGAAGATGATGAGGA	186
		Reverse	GCCAGTGAAGAGAGCCTGAC	
Rabbit Occludin	XM_008262318.1	Forward	TGGGACAGAACCTACGGAAC	134
		Reverse	GGATCCGTGTAGCCTCCATA	
Rabbit ZO-1	XM_008269782.1	Forward	GACTGATGCGAAGACGTTGA	117
		Reverse	GCAGAATGGATGCTGTCAGA	
Rabbit F-actin	XM_008265032.1	Forward	GAGCTTCATCAGCCAAGAC	125
		Reverse	CATCACCTTGCCAAGTTT	
Rabbit JAM-A	XM_008264206.1	Forward	GTAGGAAAGCCGAAGCACAG	141
		Reverse	TCAGAGGGCTCTGTCCAGTT	
Rabbit β -catenin	XM_002713075.2	Forward	CCCAGTTACCGTTCCTTCA	120
		Reverse	CAGCCCATCAACTGGGTAGT	

epithelial tissue, which could be calculated as follows:

$$R = \Delta U / \Delta I$$

The approach to calculate the resistance by applying a voltage on the tissue and measuring the resulting change in current was generally called “voltage clamping”. The output signal of electrical parameters measured by voltage/current clamp could then be visualized and recorded by a data acquisition system.

After the Ussing chamber experiments, the corneas were cut carefully to remove the scleral ring around the cornea and then stored at -80°C till the next assay.

2.3.2. Reverse transcription polymerase chain reaction (RT-PCR) assay

RNA Extraction: (1) The cornea tissues were broken by ultrasonic cell disruptor after adding 0.4 ml Trizol to release RNA and shear genomic DNA from the tissues, and then the samples were diverted into the 1.5 ml sterile RNA enzymes-free microfuge tubes. (2) 100 μl of chloroform/isoamyl alcohol (24:1, v/v) was mixed into each tube, which were blended by violent oscillation and centrifuged at 12 000 rpm (Fresco 21, ThermoFisher, USA) for 5 min. (3) The supernatant, blending with 150 μl of anhydrous ethanol, was loaded onto the adsorption columns, and wash with RPE solution twice. (4) Carefully transfer the pillars to 1.5 ml sterile RNA-enzymes free centrifuge tube, pipette 50 μl of RNase-free water onto the center of the cylindrical lining, and incubate at 80°C for 2 min. (5) Centrifuge at 10 000 rpm for 1 min, and the solution in collection tube were the RNA samples. The concentration of RNA was quantitatively determined, and the reverse transcription experiment was implemented immediately. The RNA samples should be cryopreserved at -80°C in case of failing to being used timely.

The design and synthesis of primer sequences: the primer was designed by Primer Express2.0. (ABI) software and synthesized by the Sangon Biotech (Shanghai) Co., Ltd. The sequences of primers for examined gene were shown in Table 1.

Synthesis of cDNA by reverse transcription: The experiment of RNA reverse transcription cDNA was carried out by

employing the Transcriptor First Strand cDNA Synthesis Kit in accordance with the Kit operating manual. Briefly, 1 μg total RNA and 2 μl of random primers were mixed, and add RNase-free water up to 13 μl . Add 7 μl reverse transcription mixture and incubate the reactions at 25°C for 10 min to allow primer annealing. Incubate the reactions at 55°C for 30 min to allow cDNA synthesis. Incubate the reaction at 85°C for 5 min on the thermal cycler to inactivate the reverse transcriptase to terminate cDNA synthesis.

Real-time PCR: The Real-time PCR experiments were implemented by utilizing the FastStart Universal SYBR Green Master amplification kit. The dissolution curves were also analyzed to ensure the specificity of amplification of target gene. Record the results and analyze the datum.

2.3.3. Western blot

Protein Extraction: The total proteins of corneal were extracted by use of the Total protein extraction kit. The animal tissues were blended with precooled Lysis buffer and homogenized with ultrasonic homogenizer. Then the homogenate was incubated in ice water bath for 30 min in the shaker. After being centrifuged at 12 000 rpm for 10 min at 4°C , the supernatant was obtained as the total protein samples of tissues.

Determination of total protein content: The protein determination kits of BCA method were applied to quantitative analysis the protein samples. Add the standard/samples and 200 μl BCA working liquid mixture into 96-well plates and oscillate to blend them. After incubation at 37°C for 20–30 min, the absorbance was detected on the microplate reader at 562 nm.

SDS-Polyacrylamide Gel Electrophoresis: (1) Prepare SDS-PAGE gel, which the separating gel was prepared with concentration of 8% and the stacking gel of 5%. The details were shown in Table 2. (2) 40 μg of each sample was boiled with 5 \times sample buffer for 5 min. (3) Load each sample to all wells, run the gel unit at 80 V until the samples have passed through the stacking gel for 30 min, and run at 100 V for a further 1.5 h to make sure the Marker protein is clearly separated.

Western blotting: (1) Cut the corresponding target protein gommures and soak them into the transfer buffer. At the same time, divert the PVDF membranes soaked with anhydrous

Table 2 – Preparation of SDS-PAGE gel.

	Separating gel (8%)	Stacking gel (5%)
Volume	15 ml	6 ml
40% acrylamide	3 ml	0.75 ml
Tris	3.8 ml (1.5 M, pH 8.8)	0.75 ml (0.5 M, pH 6.8)
10% SDS	0.15 ml	0.06 ml
10% AP	0.15 ml	0.06 ml
TEMED	0.009 ml	0.006 ml
ddH ₂ O	7.90 ml	4.35 ml

methanol into the transfer buffer and then transfer in ice bath. (2) Once the transfer is complete, incubate PVDF membranes in blocking buffer of PBST containing 5% skimmed milk powder for 1 h. (3) Dilute the primary antibody of proteins (claudin-1, F-actin, JAM-1, occludin, ZO-1, β -catenin) with PBST containing 5% skimmed milk powder, and add suitable amount of volume of primary antibody dilution buffer prior to rotating incubation overnight at 4 °C so as to react completely with target proteins. (4) Wash the films three times for 10 min each with PBST on a rocking platform. (5) Incubate membranes with the dilution of HRP-labeled secondary antibody for 1 h to achieve an exhaustive reaction with target proteins. Repeat the step of (4). (6) After being dry, the PVDF membrane was soaked with ECL chromogenic reagent (Chemiluminescent HRP Substrate) for 5 min to blot. (7) Imaging, fixing and film processing were carried out in a dark room. The optical density of films was analyzed using the software of NIH Image J version 1.42q to analyze and calculate the gray value in target bands, and were expressed as the ratio of grey level of target strips with GAPDH.

2.3.4. Immunofluorescence

The corneas were demounted quickly and preserved in 4% paraformaldehyde solution after Ussing chamber experiments. All resected cornea tissues were made into paraffin sections prior to immunohistochemistry assay. After dewaxing and antigen repairing, the specimens were incubated with the primary antibody and secondary antibody, respectively, and then counterstained with DAPI to stain the nucleus, sequentially. The stained samples were observed using a Nikon fluorescent microscope and photographed with a digital camera.

2.3.5. Statistical analysis

Data are presented as mean \pm SD and were compared by Student's t-test with SPSS13.0 software. $P < 0.05$ and $P < 0.01$ referred to significant and extremely significant, respectively.

3. Results and discussion

3.1. The corneal permeability of fluorescein sodium with labrasol in vitro

In order to evaluate the absorption enhancing effect of labrasol, permeability studies were performed on rabbit cornea in vitro using the Ussing chamber method. Fluorescein sodium

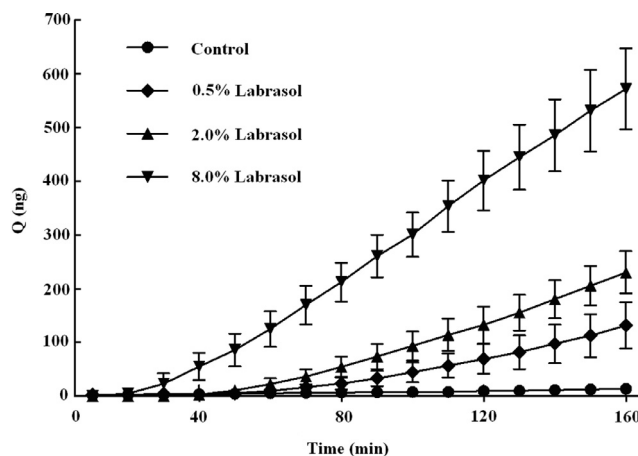


Fig. 1 – Effect of different concentrations of labrasol on the accumulative penetration amount of fluorescein sodium (mean \pm SD, $n = 6$).

Table 3 – Effect of labrasol on the permeability of fluorescein sodium (mean \pm SD, $n = 6$).

groups	Accumulative penetrated amount (ng)	$P_{app} \times 10^6$ (cm/s)
Control	13.74 \pm 5.78	2.94 \pm 1.54
0.5% Labrasol	131.51 \pm 42.93**	41.12 \pm 14.22**
2.0% Labrasol	230.34 \pm 39.31**	64.95 \pm 9.44**
8.0% Labrasol	572.22 \pm 75.65**	146.14 \pm 25.69**

Notes:
** $P < 0.01$ vs. Control

solutions with labrasol (0.5%, 2.0% and 8.0%) were added in the donor compartment separately, and their impacts on the permeability of fluorescein sodium (10 μ g/ml) could be observed as shown in Fig. 1. It was easy to note that different concentrations of labrasol distinctly promoted the transport of fluorescein sodium across the rabbit cornea, and the accumulated permeation amount increased dramatically with the increasing of the concentration of labrasol. There were significant differences between the groups with or without penetration enhancer ($P < 0.01$, Table 3). The accumulated penetration amount of fluorescein sodium with labrasol at the 160 min were 10-, 17-, 42-fold higher than that of control group, respectively.

The P_{app} value is an important parameter commonly used for the evaluation of transport processes. Calculated P_{app} values for each group were summarized in Table 3. The influences of different concentrations of labrasol on P_{app} of fluorescein sodium for corneal transport were expressed in Fig. 2. The results showed a significant difference in apparent permeability between groups with or without labrasol ($P < 0.01$). In contrast to fluorescein sodium solution group, the P_{app} increase by 14-, 22- and 50-fold respectively, with the increase of applied concentrations of labrasol (0.5%, 2.0% and 8.0%), in a concentration-dependent manner. Hence, labrasol was thought to be an effective absorption enhancer for facilitating the delivery of fluorescein sodium in rabbit cornea.

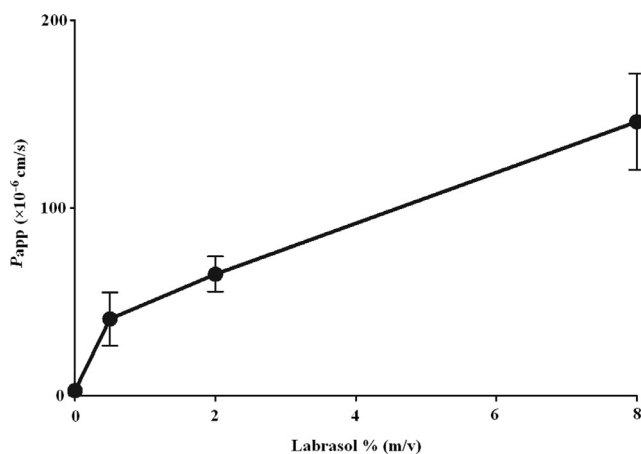


Fig. 2 – Effect of different concentrations of labrasol on the permeability of fluorescein sodium (mean \pm SD, $n = 6$).

3.2. Measurement of resistance of the cornea by Ussing chamber

The viability and integrity of tissue is particularly important for transporting drugs. Therefore, the resistance value, regarded as an indication of changes in cornea, was measured continuously at a 1 min interval during the overall process. It is a known fact that immediately after tissue insertion, the values of electrical parameters tend to oscillate. This is most often caused by the mechanical stress imposed on the samples [28]. It was crucial to confirm that the resistance values were in equilibrium to ensure the reliability of obtained data prior to the addition of applied materials. About 80 min later, the corneal resistance reached to a steady state. During the process of experiment, the resistance values were different between the groups with considerable standard deviation, which might be attributable to the individual differences in rabbit eyes. A similar phenomenon occurred in penetrated quantity of fluorescein sodium. Nevertheless, the general trend of resistance values intra-group was consistent, declining gradually with the incubation time. It was also found that corneal resistance decreased slightly after addition of fluorescein sodium and gradually returned to a time-independent steady state. In our experiments, the average resistance value of freshly excised rabbit cornea in GBR solution was in the range of approximately $800 \Omega \cdot \text{cm}^2$ – $1500 \Omega \cdot \text{cm}^2$, which was in good agreement with the previous documents [29].

Fig. 3 illustrated the effect of labrasol on the TEER of *in vitro* rabbit cornea, which has been widely recognized as an indicator for confirming tissue integrity. As Fig. 3A showed, in the blank group, the resistance of rabbit cornea exposed to GBR solution rose slowly at first and then tended to a stable state gradually. During the steady state, the resistance of rabbit cornea changed little. Interestingly, a rapid decrease in the resistance was found in the first 10 min when fluorescein sodium was added, however, the resistance recovered to a steady state value progressively (Fig. 3B). In Fig. 3C–E, the resistance value of rabbit cornea was markedly reduced after incubation with labrasol at concentrations of 0.5%, 2.0% and 8.0% (w/v). The similar results that the values of resistance re-

duce to approximately $100 \Omega \cdot \text{cm}^2$ eventually were occurred in all groups. In addition, the resistance tended to show a slow decrease in the case of exposure to 0.5% or 2.0% of labrasol. Nevertheless, 8.0% labrasol seemed to directly minimize the resistance to about $100 \Omega \cdot \text{cm}^2$ without a gradual process, suggesting that 8.0% labrasol could enhance the penetration of drugs across the cornea more efficiently. Fig. 3F displayed the profile of resistance values of 2% labrasol without fluorescein sodium. The values were close to that of 2% labrasol group (Fig. 3C) and didn't recovered to a steady state value as Fig. 3B showed, illustrating that the changing in resistance values were mainly attributed to the effect of labrasol, instead of fluorescein sodium. The profile of resistance values was incomplete and discontinuous as shown in the picture, because it was drawn by taking a data every 10 min. In essence, after the addition of penetration enhancer of labrasol, the resistance reduced continuously until it reached the minimum and maintained stable about 30 min later. The results above demonstrated that labrasol of applied concentrations could significantly reduce the rabbit corneal resistance, while fluorescein sodium resulted in a slight and reversible decrease in corneal resistance. Taken together, it could be concluded that labrasol exerted a damaged effect on corneal barrier function.

3.3. Reverse transcription polymerase chain reaction (RT-PCR) assay

The Ussing chamber experiments showed that 0.5%, 2.0% and 8.0% (w/v) of labrasol would significantly increase the cornea permeability of fluorescein sodium and significantly decrease the corneal resistance value at the same time. The effect of labrasol on mRNA expression of cytoskeleton protein F-actin, adhesion link protein β -catenin, tight junction proteins JAM-1 and claudin-1 were summarized in Table 4 and Fig. 4.

As shown in Fig. 4, the difference of F-actin mRNA expression between control group and blank group was unobvious, while in 2.0% and 8.0% of labrasol groups, the F-actin mRNA expression were differ from control group ($P < 0.05$, Table 4). It was conspicuous that labrasol group were able to down-regulate the F-actin mRNA expression in a concentration-dependent manner.

For β -catenin mRNA expression, the control group up-regulated mRNA expression of β -catenin obviously in comparison with control group. Nevertheless, 2.0% and 8.0% of labrasol groups showed obvious inhibiting effect on β -catenin mRNA expression ($P < 0.05$, Table 4), compared to control group.

It was notable that there was little difference in JAM-1 mRNA expression between control group and blank group as shown above. Furthermore, the JAM-1 mRNA expression in 0.5%, 2.0% and 8.0% of labrasol groups exhibited no significant difference compared with control group as well; indicating that mRNA expression of corneas JAM-1 protein was little influenced by the penetration enhancer of labrasol.

Compared to blank group, claudin-1 mRNA expression in control group was obviously up-regulated. However, 0.5%, 2.0% and 8.0% of labrasol groups could down-regulate the claudin-1 mRNA expression to some extent compared with control group. In addition, it was statistically significant

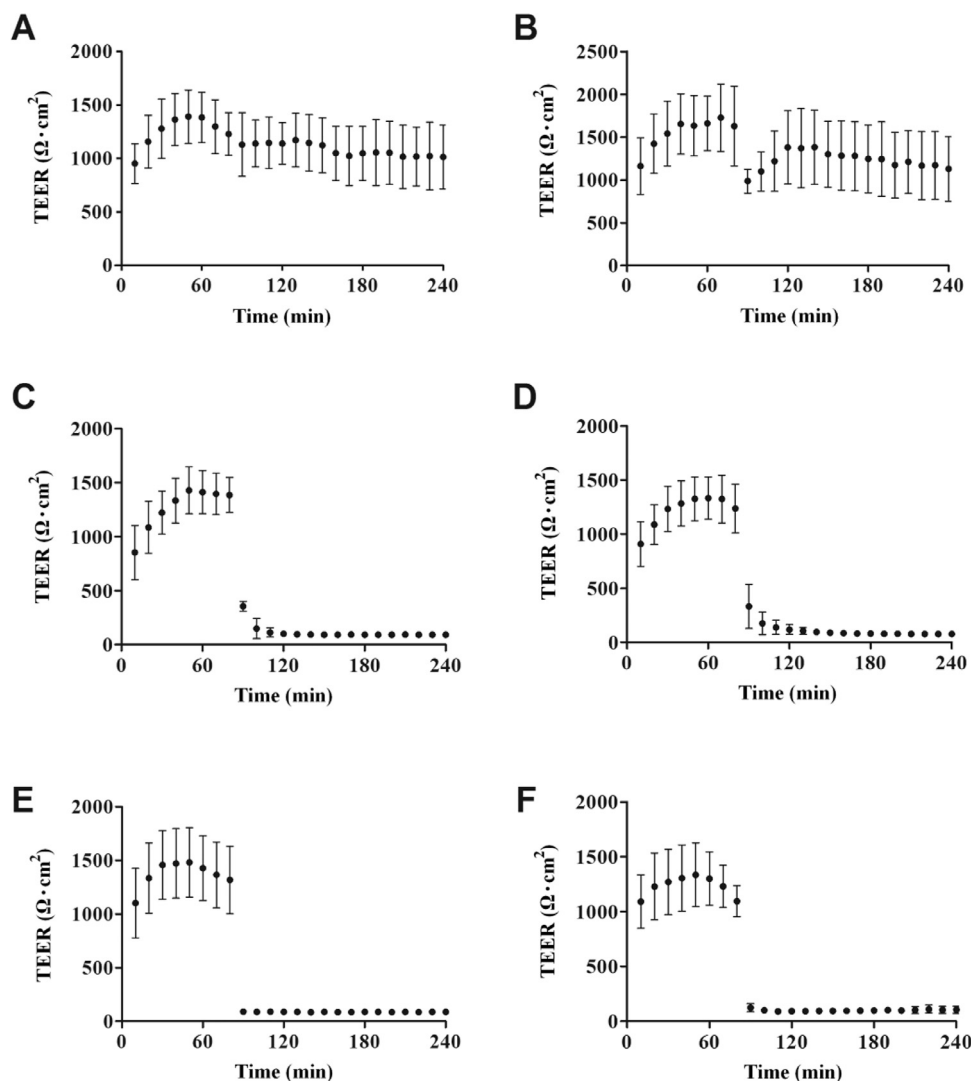


Fig. 3 – The effect of labrasol on electrical resistance of rabbit cornea. (A) Blank; (B) Control; (C) 0.5% labrasol; (D) 2% labrasol; (E) 8.0% labrasol; (F) 2% labrasol without fluorescein sodium (mean \pm SD, $n = 6$).

Table 4 – The effect of labrasol on mRNA expression of tight junction associated proteins (mean \pm SD, $n = 3$).

groups	F-actin	β -catenin	JAM-1	Claudin-1
Blank	0.96 \pm 0.14	1.03 \pm 0.04	1.07 \pm 0.16	1.07 \pm 0.11
Control	1.11 \pm 0.40	1.62 \pm 0.23 [#]	1.27 \pm 0.36	2.08 \pm 0.65
0.5% Labrasol	0.55 \pm 0.18	1.97 \pm 0.29	1.45 \pm 0.13	1.43 \pm 0.12
2.0% Labrasol	0.10 \pm 0.13 [*]	0.40 \pm 0.23 [*]	1.71 \pm 0.01	1.49 \pm 0.29
8.0% Labrasol	0.04 \pm 0.01 [*]	0.27 \pm 0.04 [*]	1.71 \pm 0.45	0.14 \pm 0.04 ^{**}

Notes:
[#] $P < 0.05$ vs. Blank.
^{*} $P < 0.05$, ^{**} $P < 0.01$ vs. Control.

($P < 0.01$) when comparing the difference of claudin-1 mRNA expression between 8.0% of labrasol group with control group.

3.4. Western blot

To demonstrate the effects of labrasol on the expression levels of several tight junction proteins, Western blotting was applied for qualitative and quantitative analysis of the four proteins. The impacts of labrasol in a series of concentrations on tight junction associated proteins expression of F-actin, β -catenin, JAM-1 and claudin-1 were described in Figs. 5, 6 and Table 5.

After the treatment of cornea with fluorescein sodium, the levels of F-actin expression was lower than blank group as Fig. 6 depicted ($P < 0.05$), indicating that exposure to fluorescein sodium might exert a certain influence on F-actin expression. Results shown in Fig. 6 indicated that protein levels were respectively reduced in response to 0.5%, 2.0% and 8.0% of labrasol, correlated with the concentration increasing of labrasol. In comparison with control group, 8.0% of labrasol exerted the strongest suppression effect on F-actin protein

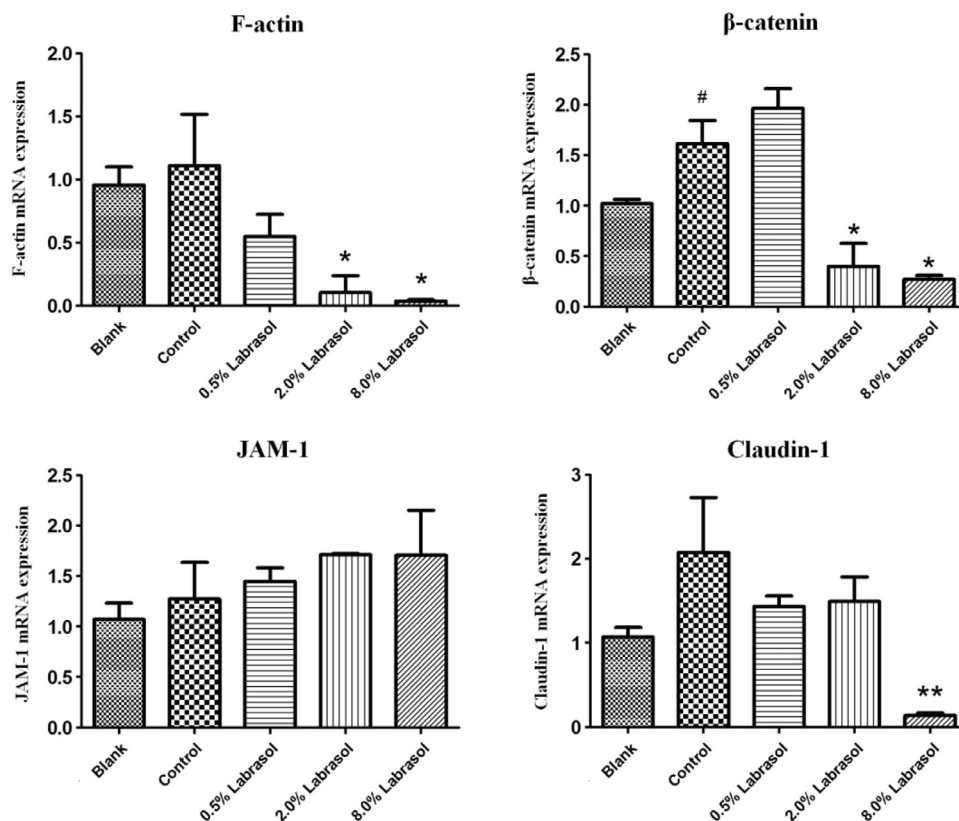


Fig. 4 – The effect of labrasol on mRNA expression of tight junction associated proteins (Mean \pm SD, $n = 3$).

Notes: # $P < 0.05$ vs. Blank; * $P < 0.05$, ** $P < 0.01$ vs. Control.

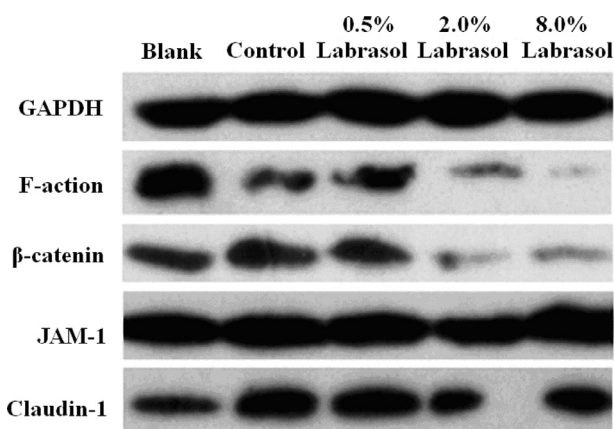


Fig. 5 – The effect of labrasol with different concentrations on expression of tight junction associated proteins.

expression ($P < 0.05$), demonstrating that labrasol contributed the most to F-actin expression at the concentration of 8.0%.

The Fig. 6 shows that β -catenin expression level in control group increased significantly ($P < 0.05$) compared to blank group, however, in contrast with control group, 0.5%, 2.0% and 8.0% of labrasol respectively repressed the β -catenin protein expression ($P < 0.05$, Table 5).

JAM-1 protein expression levels were unaltered when comparing control group with blank group. Similarly, there was

no obvious variation in JAM-1 protein expression between 0.5%, 2.0% of labrasol and the control groups. Although 8.0% of labrasol elevated JAM-1 protein expression slightly, the standard deviation was considerable, which might relate to experimental operation, and it was thought that the JAM-1 protein expression changed without variation on the whole. The results pointed that labrasol had no effect on JAM-1 protein expression.

Additionally, the control group could significantly promote the claudin-1 protein expression compared to the blank group, whereas 0.5%, 2.0% and 8.0% of labrasol separately reduced the claudin-1 protein expression ($P < 0.05$, Table 5), revealing that labrasol exerted a strong inhibitory effect on claudin-1 protein expression.

With regard to hydrophilic molecules, the transport across epithelium barrier is subject to paracellular route, which is modulated by intercellular junctional complexes. Thus, any so-called “permeation enhancer” that enhance the transport of hydrophilic drug can be assumed to exert its activity by destruction of tight connections between epithelium cells. In a negatively or positively charged SMEDDS preparation, labrasol is able to increase the paracellular transport of mannitol. It is capable of opening tight junction by modifying F-actin and ZO-1 proteins [30]. Ujhelyi et al. reported that Polyethylene glycol esters (labrasol and polysorbate 20) could influence reversibly the paracellular permeability and had impact on intestinal absorption. These surfactants have effect on tight junctions. Labrasol resulted in stronger realignment of

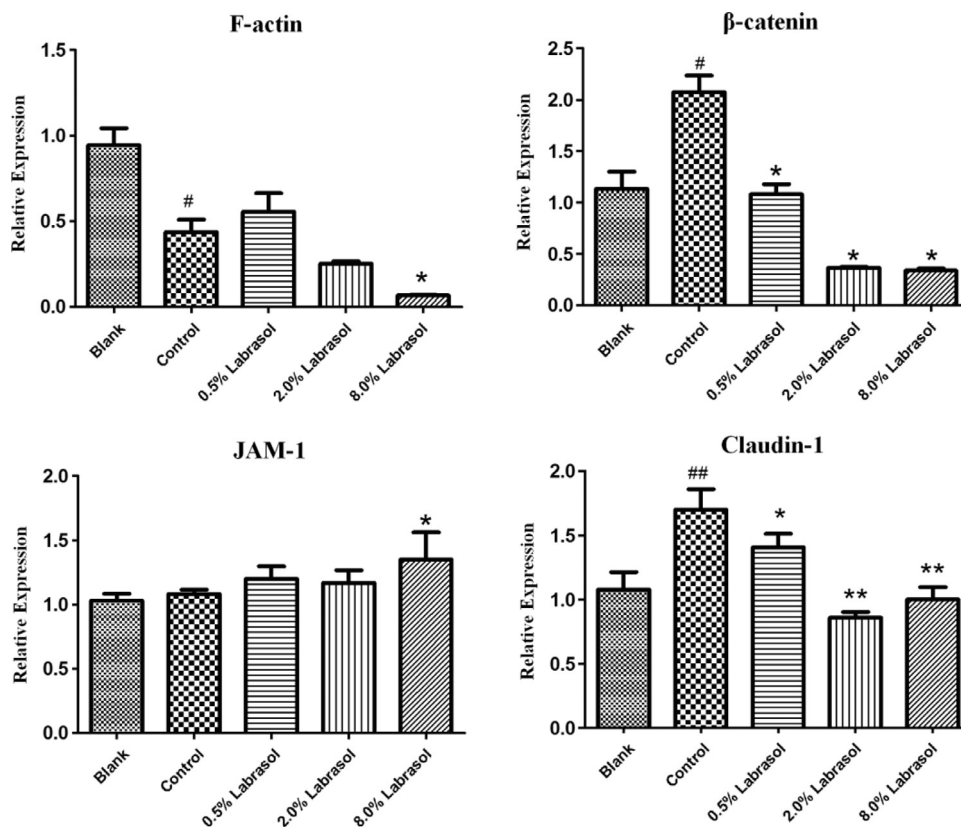


Fig. 6 – The effect of labrasol on expression of tight junction associated proteins.

Notes: [#]P < 0.05, ^{##}P < 0.01 vs. Blank; ^{*}P < 0.05, ^{**}P < 0.01 vs. Control.

Table 5 – The effect of labrasol on expression of tight junction associated proteins (mean ± SD, n = 3).

Groups	F-actin/ GAPDH	β-catenin/ GAPDH	JAM-1/ GAPDH	Claudin-1/ GAPDH
Blank	0.94 ± 0.10	1.13 ± 0.17	1.03 ± 0.05	1.08 ± 0.14
Control	0.44 ± 0.07 [#]	2.07 ± 0.17 [#]	1.08 ± 0.03	1.70 ± 0.16 ^{##}
0.5% Labrasol	0.56 ± 0.11	1.08 ± 0.10 [*]	1.20 ± 0.10	1.41 ± 0.10 [*]
2.0% Labrasol	0.25 ± 0.01	0.37 ± 0.01 [*]	1.17 ± 0.10	0.86 ± 0.05 ^{**}
8.0% Labrasol	0.07 ± 0.01 [*]	0.34 ± 0.02 [*]	1.35 ± 0.21 [*]	1.00 ± 0.10 ^{**}

Notes:

[#] P < 0.05, ^{##} P < 0.05 vs. Blank.

^{*} P < 0.05, ^{**} P < 0.01 vs. Control.

tight junction proteins (claudin-1, β-catenin and ZO-1) than polysorbate 20 [31]. Claudin-1 is a main sealing claudin in epithelia for paracellular tightness [32]. In both RT-PCR and Western blotting assays, a reduction in expression of claudin-1 was found after treating with labrasol at concentrations of 2.0% and 8.0%, compared to the control group. Goswami et al. studied disease specificity and changes in proteins pertaining to the tight junctions permeability of duodenal villi and crypts, and did not identify any role of JAM-1 in either Celiac or Crohn's diseases [33]. Our results, similar to these reports, did not identify significant alterations in JAM-1 protein expression between corneas treated with or without labrasol by either

RT-PCR or Western blotting. Therefore, JAM-1 protein expressions tended to not susceptible to labrasol and contribution of JAM-1 protein in maintenance of corneal permeability was ambiguous.

3.5. Immunofluorescence

In this experiment, we investigated immunohistochemistry of F-actin, β-catenin and claudin-1, the influences of which were confirmed in RT-PCR test and Western blot experiment.

In blank group, F-actin expression was confirmed mainly in corneal epithelium with a distribution along with the cell membrane in a net-like manner, and the intact cell morphology was obvious. Similar results were observed in control group treated with fluorescein sodium solution. The decrease of F-actin expression and blurry cell morphology shown in Fig. 7A were attributed to the application of 0.5% labrasol, which made the intracellular expression of F-actin increased. Expression of F-actin was down-regulated significantly after treating with 2.0% labrasol, and the contour of cells were illegible caused by the loss of protein with observation of decreased pericellular fluorescence. With the increase of concentration of labrasol, the expression of F-actin abated correspondingly, suggesting that labrasol was likely to influence the expression and redistribution of F-actin in a certain degree. The results in Fig. 7B showed that β-catenin was mainly present at intercellular borders in reticulate structure, encircling the cells and delineating the cellular borders, with nor-

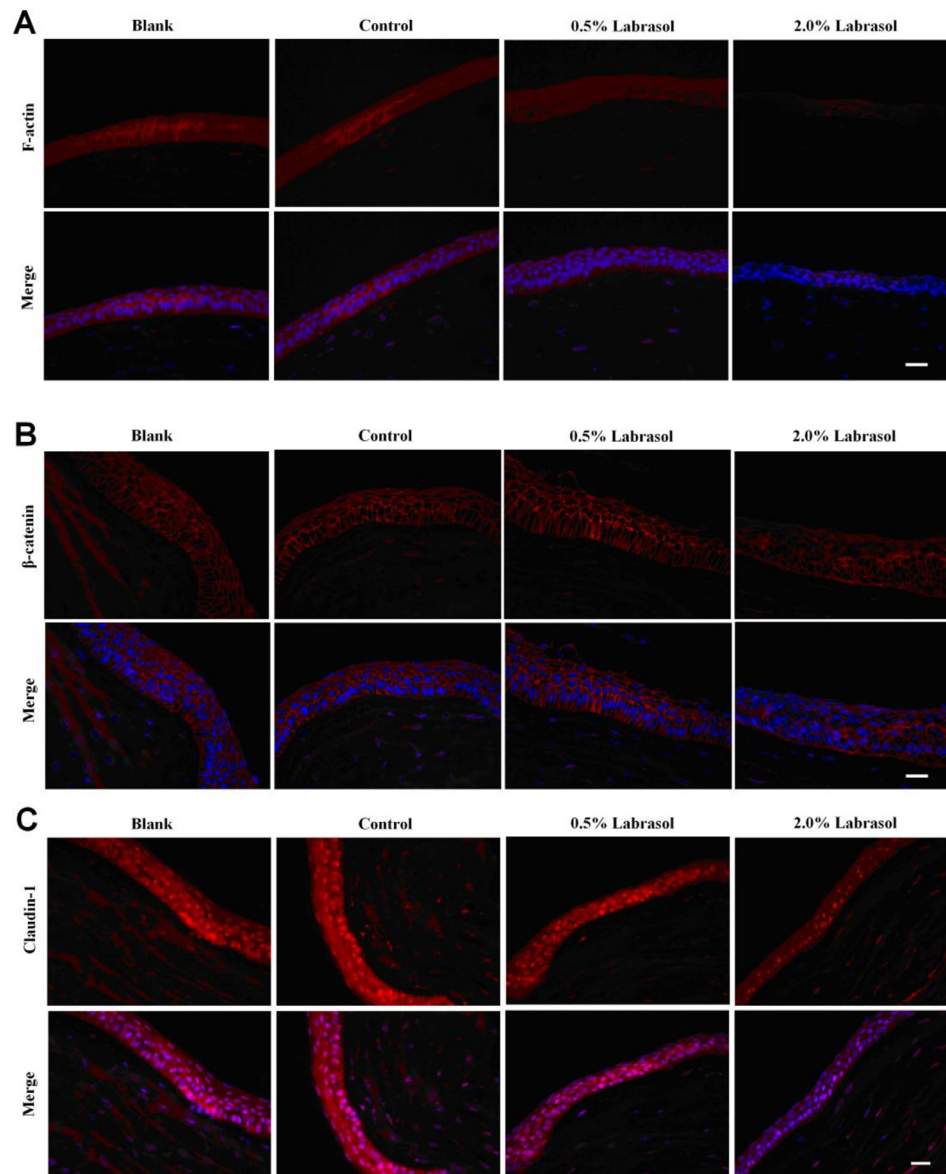


Fig. 7 – Immunohistochemistry of F-actin, β -catenin and claudin-1 influenced by labrasol. (A) The effect of labrasol on F-actin expression (B)The effect of labrasol on β -catenin expression (C) The effect of labrasol on Claudin-1 expression. Red: β -catenin, Blue: Nucleus, Scale bar: 200 μ m. (For interpretation of the references to colour in this figure legend, the reader is referred to the web version of this article.)

mal cell morphology in control group. When treated with 2.0% labrasol, the fluorescence intensity of corneal epithelial was abated, and fluorescence distribution circling the cell was discontinuous, prompting that the cell membranes appeared to be not integrated and tight junctions function was disturbed. As shown in Fig. 7C, claudin-1 expression was mainly visualized in the corneal epithelium, a little in the stromal layer as well. The claudin-1 expressed much in corneal epithelial in blank group, where the boundary between cortex layer and the substrate was clear. The control group showed an enhanced intracellular expression level of claudin-1 and epithelium integrity, while claudin-1 expression gradually weaken after being incubated with 0.5% and 2.0% of labrasol. According to the immunohistochemistry studies, intracellular junctions were disrupted and fluorescence intensity of related proteins was

decreased visibly when labrasol was employed to the *in vitro* rabbit cornea.

4. Conclusion

In summary, the study demonstrated that labrasol was capable of enhancing the excised rabbit corneal permeability for fluorescein sodium dramatically, accompanied by reduction in expression of proteins contributed to intracellular connections, which directly determined and modulated the paracellular pathways. It could be proposed that F-actin, claudin-1 and β -catenin took part in maintenance of tightness of the corneal epithelium, collectively and coordinately. Labrasol was a potent penetration enhancer for ocular drug delivery

to improve the bioavailability. One mechanisms of action was to enhance the permeability of intercellular space by down-regulating the expression level of related tight junction proteins. Much more systematic research, for instance, a range of compounds including both hydrophilic and lipophilic would be applied synchronously as model drugs to investigate the corneal penetration enhancing effects of labrasol, and also the further *in vivo* study would be required to explore insights into the complex mechanisms.

Conflicts of interest

The authors declare that there is no conflicts of interest.

REFERENCES

- [1] Gaudana R, Ananthula HK, Parenky A, Mitra AK. Ocular drug delivery. *AAPS J* 2010;12(3):348–60.
- [2] Kaur IP, Smitha R. Penetration enhancers and ocular bioadhesives: two new avenues for ophthalmic drug delivery. *Drug Dev Ind Pharm* 2002;28(4):353–69.
- [3] Xu X, Al-Ghabeish M, Rahman Z, et al. Formulation and process factors influencing product quality and *in vitro*, performance of ophthalmic ointments. *Int J Pharm* 2015;493(1-2):412–25.
- [4] Ostacolo C, Caruso C, Tronino D, et al. Enhancement of corneal permeation of riboflavin-5'-phosphate through vitamin E TPGS: a promising approach in corneal trans-epithelial cross linking treatment. *Int J Pharm* 2013;440(2):148–53.
- [5] Xiang L, Pan W, Ju C, et al. Evaluation of Pharmsolvecorneal permeability enhancement and its irritation on rabbit eyes. *Drug Deliv* 2009;16(4):224–9.
- [6] Yang H, Xun Y, Li Z, Hang T, Zhang X, Cui H. Influence of borneol on *in vitro* corneal permeability and on *in vivo* and *in vitro* corneal toxicity. *J Int Med Res* 2009;37(3):791–802.
- [7] Liu J, Fu S, Wei N, Hou Y, Zhang X, Cui H. The effects of combined menthol and borneol on fluconazole permeation through the cornea *ex vivo*. *Eur J Pharmacol* 2012;688(1-3):1–5.
- [8] Kim HJ, Yoon KA, Hahn M, Park ES, Chi SC. Preparation and *in vitro* evaluation of self-microemulsifying drug delivery systems containing idebenone. *Drug Dev Ind Pharm* 2000;26(5):523–9.
- [9] Hu Z, Tawa Rkonishi T, Shibata N, Shibata N, Takada K. A novel emulsifier, Labrasol, enhances gastrointestinal absorption of gentamicin. *Life Sci* 2001;69(24):2899–910.
- [10] Lin Y, Shen Q, Katsumi H, et al. Effects of Labrasol and other pharmaceutical excipients on the intestinal transport and absorption of rhodamine123, a P-glycoprotein substrate, in rats. *Biol Pharm Bull* 2007;30(7):1301–7.
- [11] Liu Z, Zhang X, Li J, Liu R, Shu L, Jin J. Effects of Labrasol on the corneal drug delivery of baicalin. *Drug Deliv* 2009;16(7):399–404.
- [12] Huang L, Bai J, Yang H, Liu J, Cui H. Combined use of borneol or menthol with labrasol promotes penetration of baicalin through rabbit cornea *in vitro*. *Pak J Pharm Sci* 2015;28(1):1–7.
- [13] Fu Q, Wang H, Xia M, et al. The effect of phytic acid on tight junctions in the human intestinal Caco-2 cell line and its mechanism. *Eur J Pharm Sci* 2015;80(12):1–8.
- [14] Yu N, Xun Y, Jin D, Yang H, Hang T, Cui H. Effect of sperminated pullulans on drug permeation through isolated rabbit cornea and determination of ocular irritation. *J Int Med Res* 2010;38(2):526–35.
- [15] Matter K, Balda MS. Epithelial tight junctions, gene expression and nucleo-junctional interplay. *J Cell Sci* 2007;120(Pt 9):1505–11.
- [16] Sun BO, Fang Y, Li Z, Chen Z, Xiang J. Role of cellular cytoskeleton in epithelial-mesenchymal transition process during cancer progression. *Biomed Rep* 2015;3(5):603–10.
- [17] Puthenedam M, Williams PH, Lakshmi BS, Balakrishnan A. Modulation of tight junction barrier function by outer membrane proteins of enteropathogenic *Escherichia coli*: role of F-actin and junctional adhesion molecule-1. *Cell Biol Int* 2007;31(8):836–44.
- [18] Tebbe B, Mankertz J, Schwarz C, et al. Tight junction proteins: a novel class of integral membrane proteins. *Arch Dermatol Res* 2002;294(1-2):14–18.
- [19] Haseloff RF, Dithmer S, Winkler L, Wolburg H, Blasig IE. Transmembrane proteins of the tight junctions at the blood-brain barrier: structural and functional aspects. *Semin Cell Dev Biol* 2015;38:16–25.
- [20] Citi S. The molecular organization of tight junctions. *J Cell Biol* 1993;121(3):485–9.
- [21] Balda MS, Matter K. Tight junctions at a glance. *J Cell Sci* 2008;121(22):3677–82.
- [22] Tscheik C, Blasig IE, Winkler L. Trends in drug delivery through tissue barriers containing tight junctions. *Tissue Barriers* 2013;1(2):e24565.
- [23] Dabrowski S, Staat C, Zwanziger D, et al. Redox-sensitive structure and function of the first extracellular loop of the cell-cell contact protein claudin-1: lessons from molecular structure to animals. *Antioxid Redox Signal* 2015;22(1):1–14.
- [24] Liu Y, Nusrat A, Schnell FJ, et al. Human junction adhesion molecule regulates tight junction resealing in epithelia. *J Cell Sci* 2000;113(Pt 13)(13):2363–74.
- [25] Niessen CM. Tight junctions/adherens junctions: basic structure and function. *J Invest Dermatol* 2007;127(11):2525–32.
- [26] Harris TJ, Tepass U. Adherens junctions: from molecules to morphogenesis. *Nat Rev Mol Cell Biol* 2010;11(7):502–14.
- [27] Tietz S, Engelhardt B. Brain barriers: Crosstalk between complex tight junctions and adherens junctions. *J Cell Biol* 2015;209(4):493–506.
- [28] Li H, Sheppard DN, Hug MJ. Transepithelial electrical measurements with the Ussing chamber. *J Cyst Fibros* 2004;3(3):123–6.
- [29] Bonanno JA. Identity and regulation of ion transport mechanisms in the corneal endothelium. *Prog Retin Eye Res* 2003;22(1):69–94.
- [30] Sha X, Yan G, Wu Y, Li J, Fang X. Effect of self-microemulsifying drug delivery systems containing Labrasol on tight junctions in Caco-2 cells. *Eur J Pharm Sci* 2005;24(5):477–86.
- [31] Ujhelyi Z, Fenyvesi F, Váradi J, et al. Evaluation of cytotoxicity of surfactants used in self-micro emulsifying drug delivery systems and their effects on paracellular transport in Caco-2 cell monolayer. *Eur J Pharm Sci* 2012;47(3):564–73.
- [32] Zwanziger D, Hackel D, Staat C, et al. A peptidomimetic tight junction modulator to improve regional analgesia. *Mol Pharm* 2012;9(6):1785–94.
- [33] Goswami P, Das P, Verma AK, et al. Are alterations of tight junctions at molecular and ultrastructural level different in duodenal biopsies of patients with celiac disease and Crohn's disease. *Virchows Arch* 2014;465(5):521–30.